Internal-Conversion Electrons Emitted by Different Elements in the Fission of Cf^{252}†*

N. L. Shapiro,‡ B. W. Wehring, and M. E. Wyman
Nuclear Engineering Program, University of Illinois, Urbana, Illinois 61801
(Received 17 August 1970)

Coincidence measurements of the internal-conversion electrons and x rays emitted by the fragments and products of the spontaneous fission of Cf^{252} are reported. In the experiment, two-parameter data were recorded event by event and stored sequentially on magnetic tape. The first parameter contained information on the energy of the x ray as measured by a high-resolution semiconductor detector and was used to determine the atomic number of the de-exciting nucleus. The second parameter contined information on the energy of the internal-conversion electrons. Two measurements were performed. The first measurement recorded only electrons emitted from the pre-β-decay fission fragments, while the second measured events from both the fragments and products of fission. In general it was found that the x rays from an element are produced by numerous internal-conversion transitions. The energies of these transitions are tabulated for each element produced in fission. A greater number of these transitions were observed to occur for odd-Z elements than for even-Z elements suggesting the even-even nuclides contribute little to the x-ray spectrum. This even-odd effect was more pronounced in the measurement of events from both fragments and products of fission than in the measurement of events from the fission fragments alone.

I. INTRODUCTION

The fission of a heavy nucleus normally produces two fission fragments which are highly excited and far from β stability. These fragments deexcite first by the emission of neutrons and then by γ decay. Most of the fragments are still neutron-rich and suffer a series of β decays (approximately three) to reach stability. Usually the β decays are to excited levels in the daughters (fission products) with subsequent γ decays and, in rare cases, neutron emission. Often the lower-energy γ transitions in both the fragments and decay products are internally converted in the K electron shell. The electron vacancy produced by the internal-conversion process is most often filled by an L shell electron with the resulting emission of a $K\alpha$ x ray.

Most experiments measuring K x-ray yields have been performed using NaI(Tl) scintillators or proportional counters. Measurements employing the spontaneous fission of Cf^{252} have produced x-ray yields and energy spectra associated with specific fission-fragment mass intervals.[1-3] Similar measurements have been performed for the thermal-neutron fission of U^{235}.[4,5] These studies have provided a great deal of information about the general features of the nuclear structure of the fission fragments.

The use of high-resolution x-ray spectrometers allows the x-ray yields to be measured for each element produced by fission and affords the opportunity to realize more detailed information on the nuclear structure of the fragments. Initial high-resolution measurements of the K x rays were made using bent-crystal spectrometers. Studies of the x rays from heavy fragments and β-decay products of U^{235} were made using transmission-type bent-crystal spectrometers.[6-8] A measurement of K x rays in coincidence with the thermal fission of U^{235} using a reflection-type bent-crystal spectrometer was also made.[9] Unfortunately, the low efficiencies associated with dispersive spectrometers makes their use in coincidence experiments impractical.

The improvement in the performance of semiconductor detectors and low-noise electronics has made high-resolution coincidence experiments feasible. The x-ray yields as a function of atomic number for the spontaneous fission of Cf^{252},[10] and both the total x-ray yields and the x-ray yields for selected mass intervals for the thermal-neutron fission of Pu^{239}, U^{235}, and U^{233} [11] have been measured using high-resolution semiconductor detectors.

Studies of the internal conversion electrons from fission have been less frequent. Bowman, Thompson, Watson, Kapoor, and Rasmussen,[1] and Atneosen and Thomas[12] have measured internal conversion electron spectra associated with specific fission-fragment mass intervals. More recently Watson, Wilhelmy, Jared, Rugge, Bowman, Thompson, and Rasmussen[13] have measured the energies of coincident complementary fragment pairs, internal conversion electrons, and K x rays from the fission of Cf^{252}. This experiment, which measured events occurring within a few nsec of fission, determined the atomic numbers and weights of fragments associated with a large number of low-energy transitions.

In the present experiment, the internal conversion electron spectrum in the range of 100 keV to 1 MeV was measured for each element produced in the spontaneous fission of Cf^{252} using a high-resolution semiconductor detector. The Z of the nucleus undergoing internal conversion was determined by measuring the energy of the x ray. A semiconductor detector which had sufficiently good resolution to distinguish the characteristic x-ray lines from adjacent Z elements was used. Thin plastic scintillators were used to detect the fission event and to stop the fission fragments.

In previously reported work, electrons emitted by fission fragments were measured while the fragments were still in motion. Extremely low-energy electrons could be detected since there was no material between the fragment and detector to absorb the electron or to degrade its energy. The resolution of such an experiment for high-energy electrons, however, is limited because of Doppler broadening of the electron lines due to fragment motion. The x-ray resolution is also degraded by Doppler broadening with the result that at reasonable detection efficiencies the characteristic x rays of light fragments were not completely resolved.

In the present experiment, the fragments were stopped in the scintillators in times shorter than that characteristic of the internal conversion process, and hence Doppler broadening of the electron and x-ray lines was all but eliminated. This experiment is thus able to measure high-energy electron transitions, such as those expected from many even-even nuclides. The degradation of electron energy in the scintillators does, however, limit the experiment to the measurement of transitions above 100 keV. The elimination of Doppler broadening also allows the characteristic x rays from adjacent Z elements to be resolved over the entire range of interest. The resolution of adjacent x-ray lines is necessary in this type of measurement since the electron data must be sorted by element in order to resolve electron lines. Sorting by element also has the advantage that the atomic number of the emitting fragment can be assigned even to unresolved electron lines. This experiment is also unique in that the data are not biased by a preferential time interval. In experiments measuring electrons and x rays from moving fragments, the period of observation is limited by the length of the flight path and typically only events occurring within the first few nsec are observed. The detection efficiency also is dependent upon the time of emission. In the present experiment, events from the act of fission to an arbitrary time were measured with uniform efficiency.

Two separate measurements were performed. In the first, the x-ray–electron–fission coincident experiment, the energies of the internal-conversion electrons and x rays emitted from pre-β-decay fragments were recorded event by event. The second experiment, the x-ray–electron coincident experiment, measured electrons and x rays from both the fission fragments and the decay products. The energy assignments for these two sets of measurements are given in Tables I and II.

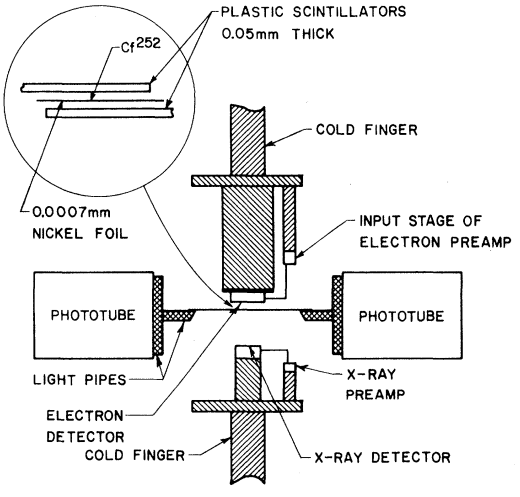

FIG. 1. Schematic drawing of the geometry used in the experiment. Si(Li) semiconductor detectors view x rays and electrons from a Cf^{252} source sandwiched between two plastic scintillators which serve both to detect and stop the fission fragments.

II. EXPERIMENTAL SYSTEM

The experimental arrangement for the measurement of the energies of the internal-conversion electrons and the resulting x rays emitted in fission is shown schematically in Fig. 1. Figure 2 is a block diagram of the electronics used in the experiment.

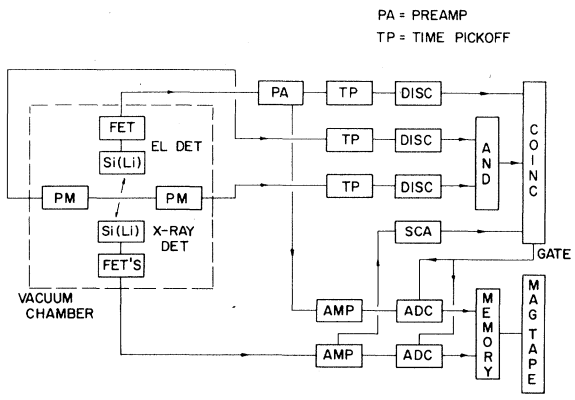

FIG. 2. Block diagram of the electronics used in the experiment.

TABLE I. Energy assignments of observed lines for the x-ray–electron–fission measurement.

Z	Channel	E_e (keV)	E_γ (keV)	Comments
38	67	168 ± 5	184 ± 5	
39	45	118 ± 5	135 ± 5	
	89	218 ± 7	235 ± 7	
	110	265 ± 7	283 ± 7	
	146	345 ± 6	362 ± 6	
40	38–46	102–120	120–138	Complex
	79	195 ± 5	213 ± 5	$A \pm 2 = 98$, $A \pm 1 = 102$, [a] $A \pm 1 = 100$ [b]
	101	243 ± 5	261 ± 5	
	371	845 ± 3	863 ± 3	
41	79	195 ± 5	214 ± 5	
	97	235 ± 5	254 ± 5	
	190–220	440–510	459–529	Complex
	240	555 ± 10	574 ± 10	
42	58	150 ± 5	170 ± 5	$A \pm 1 = 106$ [a, b]
	68	170 ± 5	190 ± 5	$A \pm 1 = 106$, [a] $A \pm 1 = 104$ [b]
44	44	116 ± 3	138 ± 4	
	66	165 ± 5	187 ± 5	
	90	219 ± 5	241 ± 5	Strong, $A \pm 1 = 110$ [c] $A \pm 2 = 109$, [d] $A \pm 1 = 110$ [a] $A \pm 1 = 108$, 110, 112 [b]
	102	245 ± 7	267 ± 7	
	143	340 ± 7	362 ± 7	
	194	452 ± 3	474 ± 3	
	209	487 ± 8	509 ± 8	$A \pm 1 = 110$ [c]
	216	505 ± 7	527 ± 7	$A \pm 1 = 110$ [c]
	231	537 ± 7	559 ± 7	
45	50	130 ± 5	153 ± 5	$A \pm 1 = 112$ [c]
	73	180 ± 10	203 ± 10	
	100	240 ± 12	263 ± 12	
46	52	133 ± 7	157 ± 7	
	85	208 ± 12	232 ± 12	
	115	274 ± 7	299 ± 7	
	132	312 ± 12	336 ± 12	$A \pm 1 = 112$, 114, 116 [c]
47	50	130 ± 5	156 ± 5	
	57	145 ± 5	171 ± 5	
	68	170 ± 5	196 ± 5	
48	63	159 ± 7	186 ± 7	
	81	199 ± 5	226 ± 5	
	95	230 ± 4	256 ± 4	
49	125	297 ± 10	325 ± 10	
50	40	110 ± 7	139 ± 7	
	52	133 ± 5	162 ± 5	
51	47	122 ± 5	152 ± 5	
	62	156 ± 5	186 ± 5	
52	42	111 ± 7	143 ± 7	
	55	140 ± 3	172 ± 7	
	111	268 ± 5	300 ± 7	
53	54	140 ± 7	173 ± 7	
54	34	92 ± 3	127 ± 3	
	42	111 ± 5	146 ± 5	
	120	287 ± 5	322 ± 5	
	148	350 ± 7	385 ± 7	$A \pm 1 = 139$ [c]
	193	450 ± 7	485 ± 7	$A \pm 1 = 140$, 142 [c]
	240	555 ± 7	590 ± 7	Complex, $A \pm 1 = 139$ [c]
	254	589 ± 7	626 ± 7	

TABLE I *(Continued)*

Z	Channel	E_e (keV)	E_γ (keV)	Comments
55	68	170 ± 3	206 ± 3	$A \pm 1 = 142, 145$,[c] 142[e]
	137	325 ± 5	361 ± 5	$A \pm 1 = 140$[c]
	250	575 ± 7	611 ± 7	$A = 139$[e]
	330	760 ± 7	796 ± 7	$A = 140$[e]
56	62	157 ± 5	194 ± 5	$A = 144 \pm 1$[a]
	126	300 ± 5	337 ± 5	Complex
	137	320 ± 5	357 ± 5	Complex, $A \pm 1 = 144$[c], 142[e]
	165	388 ± 7	425 ± 7	$A = 142$[e]
	177	415 ± 7	452 ± 7	
	195	454 ± 7	491 ± 7	
	253	588 ± 7	625 ± 7	$A = 142$[e]
	282	650 ± 7	687 ± 7	
	298	684 ± 7	721 ± 7	
	326	750 ± 10	787 ± 10	
	357	820 ± 7	857 ± 7	
57	44	117 ± 3	156 ± 3	$A \pm 2 = 145$[d]
	53	137 ± 5	176 ± 5	$A \pm 2 = 145$[d]
	82	200 ± 7	239 ± 7	$A \pm 2 = 147$,[d] $A \pm 2 = 146$[a]
	103	250 ± 5	289 ± 5	
	113	270 ± 5	309 ± 5	
	235	547 ± 12	586 ± 12	
	246	568 ± 12	607 ± 12	
	325	747 ± 12	786 ± 12	
	365	838 ± 12	877 ± 12	
	433	990 ± 12	1029 ± 12	
58	41	110 ± 5	150 ± 5	
	145	342 ± 7	382 ± 7	
	208	482 ± 7	522 ± 7	
59	43	114 ± 5	156 ± 5	
	52	135 ± 5	177 ± 5	
	100	240 ± 7	282 ± 5	
	214	499 ± 12	541 ± 12	
60	40	108 ± 7	152 ± 7	
	61	154 ± 5	198 ± 5	
	72	180 ± 5	224 ± 5	
	82	200 ± 5	244 ± 5	
	106	255 ± 7	299 ± 7	
61	96	232 ± 7	277 ± 7	
	110	265 ± 10	310 ± 10	
	142	335 ± 7	380 ± 7	
62	65	162 ± 7	209 ± 7	
	85	210 ± 5	257 ± 5	

[a] Tentative assignment of A based on work of Watson *et al.* (Ref. 13).
[b] Tentative assignment of A based on work of Cheifetz *et al.* (Ref. 19).
[c] Tentative assignment of A based on γ and electron transitions observed by Bowman *et al.* (Ref. 1).
[d] Tentative assignment of A based on electron transitions observed by Atneosen *et al.* (Ref. 12).
[e] Tentative assignment of A based on γ transitions observed by T. Alvager, R. A. Naumann, R. F. Petry, G. Sidenius, and T. Darrah Thomas, Phys. Rev. 167, 1105 (1968).

The x-ray detection system consisted of a high-resolution lithium-drifted semiconductor detector, preamplifier, amplifier, analog-to-digital converter (ADC), and timing electronics. The detector, which was made in our laboratory, had an area of 125 mm^2 and a depletion depth of 4 mm. The detector was dc coupled to the input of a voltage-sensitive field-effect-transistor (FET) preamplifier.[14] The preamplifier, consisting of two ac-coupled FET's, was mounted in its entirety on the x-ray detector holder (Fig. 1). Both the detector and the preamplifier were cooled by liquid nitrogen. The x-ray pulse heights were digitized by an ADC employing 1024-channel resolution. Timing pulses of the zero-crossover type were derived from the x-ray pulse after the pulse had been amplified and differentiated, but prior to integration. This arrangement permitted proper gating of the ADC's while minimizing the possibility of introducing noise into the system.

TABLE II. Energy assignments of observed lines for the x-ray–electron measurement.

Z	Channel	E_e (keV)	E_γ (keV)	Comments
39	51	131 ± 7	148 ± 7	
	129	307 ± 5	324 ± 7	
40	131	311 ± 5	329 ± 5	
	371	845 ± 3	863 ± 3	
42	300	690 ± 7	710 ± 7	
	316	725 ± 3	745 ± 3	Strong
43	67	167 ± 7	189 ± 7	
	134	320 ± 7	341 ± 7	
46	102	246 ± 7	370 ± 7	
	152	360 ± 7	384 ± 7	
	170	400 ± 7	424 ± 7	
47	131	310 ± 5	336 ± 5	
49	120	287 ± 3	315 ± 3	$A = 117$ [a]
	130	307 ± 3	335 ± 3	Strong, $A = 115$ [a]
50	62	157 ± 5	186 ± 5	
51	38	101 ± 5	131 ± 5	
	135	320 ± 7	350 ± 7	
	155	367 ± 7	397 ± 7	
53	76	190 ± 7	223 ± 7	
	95	230 ± 7	263 ± 7	
	128–138	304–328	337–361	Complex
54	61	152 ± 3	187 ± 3	
	215	500 ± 3	535 ± 3	Strong
55	41	110 ± 3	146 ± 3	
	87	212 ± 5	248 ± 5	$A = 135$ [a]
	308	710 ± 7	746 ± 7	$A = 138$ [b]
56	242	560 ± 7	597 ± 7	$A = 140$ [b]
57	86	210 ± 5	249 ± 5	
	257	597 ± 7	636 ± 7	
58	96	230 ± 5	270 ± 5	
	153	361 ± 7	401 ± 7	

[a] Tentative assignment of A based on decay schemes of C. M. Lederer, J. M. Hollander, and I. Perlman, *Table of Isotopes* (John Wiley & Sons, Inc., New York, 1968).

[b] Tentative assignment of A based on the γ transitions observed by Alvager *et al.* (Ref. e of Table I).

The x-ray system showed an energy resolution of 590 eV full width at half maximum for the 22.1-keV x ray produced in the decay of Cd^{109}. In the experiment the resolution performance is somewhat degraded due to pulse pileup of the signal with pulses produced by high-energy prompt fission γ rays. These high-energy pulses saturate the amplifier and produce large undershoots which take a relatively long time to decay to the baseline. As a consequence, some degradation in resolution occurs even at the relatively low count rate employed in the experiment of 1000 counts/sec. Under experimental conditions, the system showed a resolution of 620 eV for the 15-keV x rays from the Cf^{252} source. This resolution is sufficient to resolve the characteristic x-ray lines from elements of adjacent Z.

The internal-conversion-electron spectrum was measured by a high-resolution lithium-drifted semiconductor detector which had an area of 100 mm^2 and a depletion depth of 2 mm. The 2-mm depletion depth allowed electrons of 1 MeV or less energy to be stopped in the detector. The detector was ac coupled to the input stage of an FET preamplifier. Both the detector and the FET input stage were mounted on the detector holder and were cooled to liquid-nitrogen temperature. The electron pulse heights were digitized by an ADC employing 4096-channel resolution. Timing pulses of the zero-threshold type were generated by a time pickoff connected to the output of the preamplifier. The electron system showed resolutions of 3.5 keV for 976-keV electrons and 3.0 keV for 482-keV electrons produced in the decay of Bi^{207}.

The spontaneous fission of Cf^{252} was used as the fission source. A source of 500 fissions/sec was self-transferred onto a nickel foil of 0.0007-mm thickness. This foil was sandwiched between two plastic scintillators of 0.05-mm thickness.[15] The scintillators served both to detect fission and to stop the fission fragments. Since the fragments were stopped within approximately 5×10^{-12} sec of fission, broadening of the x-ray and electron lines by Doppler broadening was all but eliminated.

Light produced in the scintillators was internally reflected down the length of the scintillators, into light pipes, and onto the cathodes of the photomultipliers. The two scintillators were optically isolated from each other by the source foil. The performance of both scintillators was monitored by observing the amplified output pulses of each pho-

tomultiplier using a 400-channel analyzer.

Due to the large pulse-height defect of the scintillators for heavy ions, the α peak from the α decay of Cf^{252} is more or less superimposed upon the heavy-fragment peak. As a consequence, it is necessary to require a coincidence output from both scintillators to determine a fission event. Timing pulses of the zero-threshold type were generated by time pickoffs connected to the anodes of the photomultiplier. Since there are approximately 32 α decays per fission decay of Cf^{252}, the singles rate in each scintillator is large. In order to minimize accidental coincidences, a coincidence resolving time of $2\tau = 30$ nsec was employed.

The response of the electron detection system to electrons produced by the fission source is complicated. Since the fission fragments are stopped within the plastic scintillators, the electrons are emitted from within the scintillators and consequently suffer an energy loss as they pass through the plastic. The energy spectrum of initially monoenergetic electrons after having passed through a thickness of material has been calculated by Williams[16] and Landau.[17] The spectrum is usually described in terms of the sum of two contributions: (1) a Gaussian produced by soft collisions in which the incident electron loses only a small fraction of its energy (the mean energy is shifted downward somewhat from the initial energy), and (2) a tail produced by the infrequent occurrence of hard collisions in which a large fraction of the energy is lost. The mean energy of the Gaussian, the standard deviation of the Gaussian, and the ratio of soft-to-hard collisions is a function of the energy of the incident electrons and the thickness of the material through which they pass.

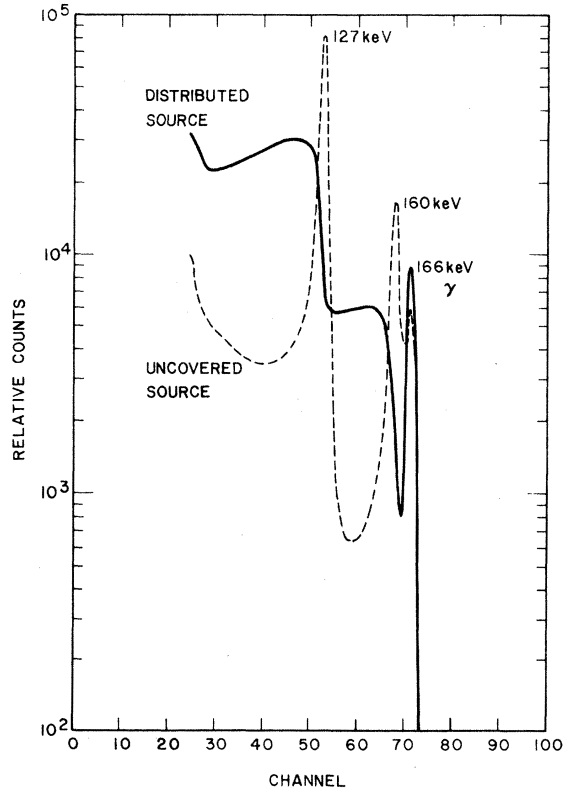

FIG. 3. Comparison of the Ce^{139} internal-conversion-electron spectrum from an uncovered source and the distributed source.

In the case of the fission source, electrons must pass through a thickness of material which depends on the position in the scintillator of the stopped fragment. In order to obtain some insight into the shapes of the electron spectra from the fission source, the electron spectra of Bi^{207}, Sn^{113}, and Ce^{139} were measured from distributed sources constructed of eight layers of 0.012-mm Mylar. An equal amount of the isotope under study was deposited on each of the layers of Mylar. For Bi^{207} and Sn^{113} the resolution was degraded with the addition of a tail on the low-energy side of the peak. The magnitude of the tail increases as the energy of the electrons decreases. Figure 3 compares the spectra obtained from an uncovered source with that from the distributed source for the 160- and 127-keV electrons from the decay of Ce^{139}. These monoenergetic electrons appear as edges in the distributed source spectrum due to the large tails on the low-energy side of the peak; however, the high-energy edge remains relatively sharp. Figure 4 shows a similar measurement for the decay of Bi^{207}, and illustrates the improvement in resolution and peak shape for higher-energy transitions.

III. EXPERIMENTAL PROCEDURE

The energies of an electron and an x ray were digitized by the ADC's, and the magnitude of each pulse was recorded event by event in a buffer memory. After 501 events were recorded in the buffer memory, the contents of the memory were transferred onto computer-compatible magnetic tape.

In the x-ray–electron–fission coincident measurement, the energies of the electron and the x ray were recorded if the electron and x ray were emitted within 0.5 μsec of each other and within 1.5 μsec of fission. This measurement ran for a period of 45 days in which 3.0×10^6 events were recorded and analyzed. The data were collected in three runs. Each run was analyzed individually, and then the results of the three runs were combined.

In the second measurement, the x-ray–electron coincident measurement, the electrons and x rays were not required to be in coincidence with fission.

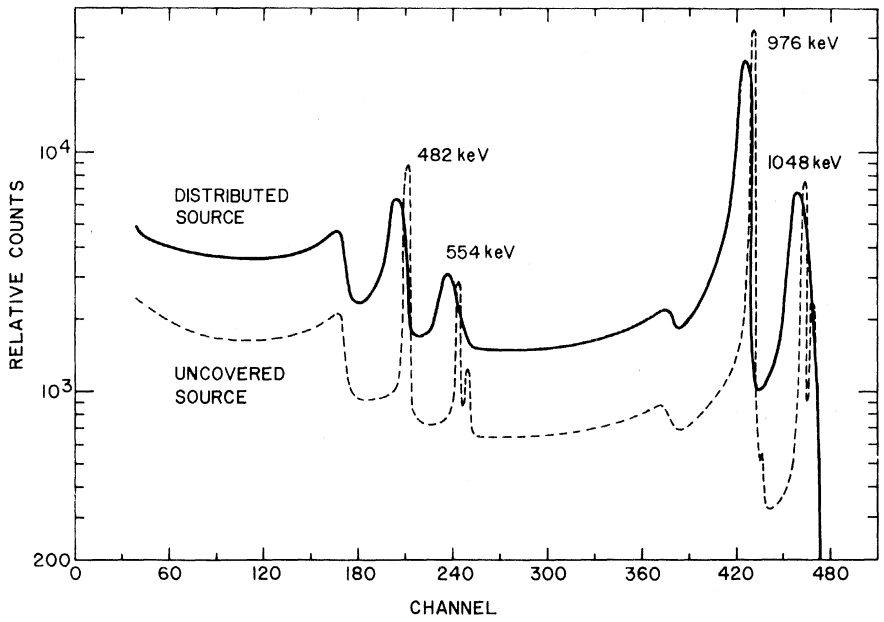

FIG. 4. Comparison of the Bi^{207} internal-conversion-electron spectrum from an uncovered source and the distributed source.

In this measurement, the energies of the electrons and x rays were recorded if the electron and x ray were emitted within 0.25 μsec of each other. The experiment was run continuously for 7 days and a total of 3.5×10^6 events were recorded and analyzed.

The long period of time necessary to collect the data required that both the zero level (slope intercept) and the gain of the system be digitally stabilized to prevent gain drifts in the system from dispersing the resolution. The gain of the x-ray system was stabilized by using the cesium x-ray peak from fission. Since there is no intense peak in the unsorted electron spectrum, the gain of the elec-

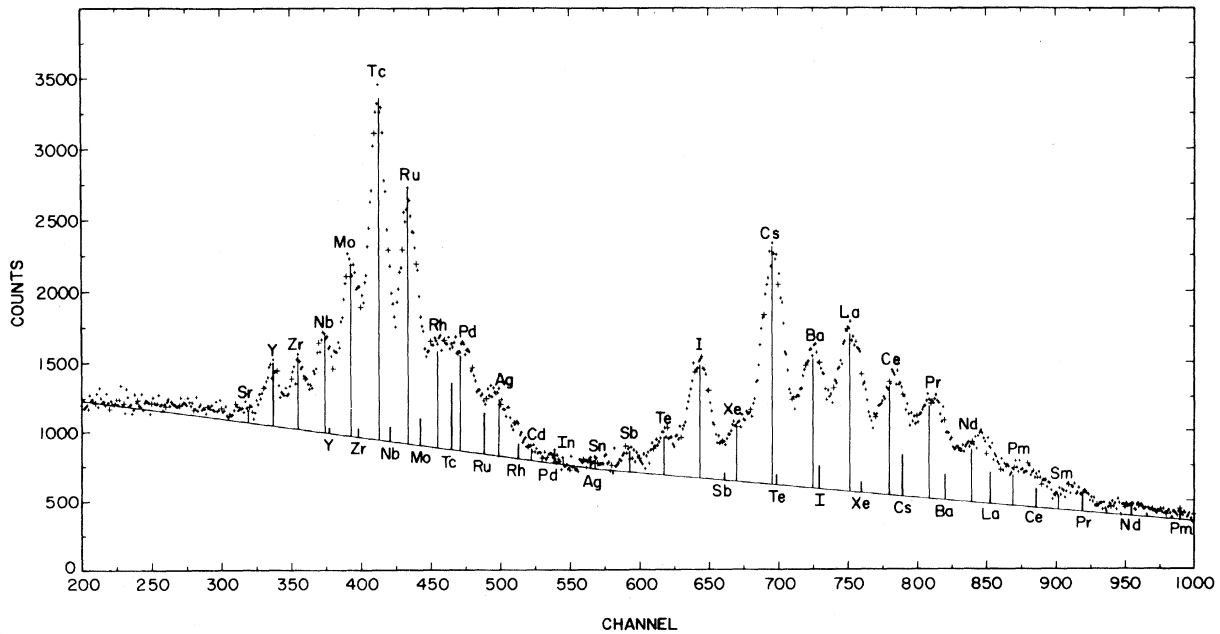

FIG. 5. X rays in coincidence with fission of Cf^{252}. The energy calibration is 44.3 eV/channel. The thin lines represent the $K\alpha$ emission and the thick lines represent the $K\beta$ emission. The heights of these lines are proportional to the yields of the x rays.

tron system was stabilized on a peak provided by a pulser connected to the input of the preamplifier.

The calibration procedure for both experiments was the same. The x-ray system was calibrated using the x rays emitted in coincidence with fission. The atomic number of the nucleus associated with each peak in the x-ray spectrum was assigned by using the Cm L x rays resulting from the α decay of the Cf^{252} source. The electron system was calibrated using the 976- and 482-keV internal-conversion electron lines from the decay of Bi^{207}, the 364-keV internal-conversion line from the decay of Sn^{113}, the 160-keV internal-conversion line from the decay of Ce^{139}, and the 84.2- and 62.2-keV internal-conversion lines from the decay of Cd^{109}.

IV. RESULTS

A. X-Ray Spectra

The spectrum of x rays which are in coincidence with fission of Cf^{252} is shown in Fig. 5. The atomic number of each peak observed in the spectrum and the channel numbers corresponding to the energies of each $K\alpha$ x ray and each $K\beta$ x ray were assigned by using the Cm L x rays from the Cf^{252} source for calibration. This calibration was confirmed by comparison to the work of Watson.[10] The heights of the $K\beta$ x-ray peaks were calculated using the ratio of intensities of the $K\alpha$ to $K\beta$ x rays given by Wapstra, Nijgh, and Van Liehout.[18] This was done only to give an approximate indication of how the $K\alpha$ and $K\beta$ lines add together to give the observed peaks. No attempt was made to correct these results for the variation in detector efficiency or the lack of filled M shells which occur in many of the fragments.

Figure 6 shows the spectrum of x rays which are in coincidence with both fission of Cf^{252} and electrons above approximately 50 keV. Figures 5 and 6 show essentially the same features and the similar relative intensities of the x rays indicate that preferential discrimination against low-energy electrons has little effect on the x-ray spectrum.

The spectrum of x rays in coincidence with electrons above 50 keV is shown in Fig. 7. Since the x rays are not required to be in coincidence with fission, both the prompt x rays and x rays produced by the β-decaying fragments are observed. This spectrum shows a significant change in the general features as compared to Figs. 5 and 6 which show only a slight indication of an even-odd effect with a low x-ray yield for the even-Z elements xenon and barium. Similar even-odd effects were observed by Watson, Bowman, and Thompson[10] for x rays from Cf^{252} fragments. The effect is much more pronounced for the x-ray spectrum shown in Fig. 7, where the intensities of the odd-Z elements antimomony, iodine, cesium, lanthanum, and praseodymium are noticeably more intense than their even-Z neighbors. A similar pronounced even-odd effect was observed by John, Massey, and Saunders[7] for the x rays emitted from fission fragments and products of the ther-

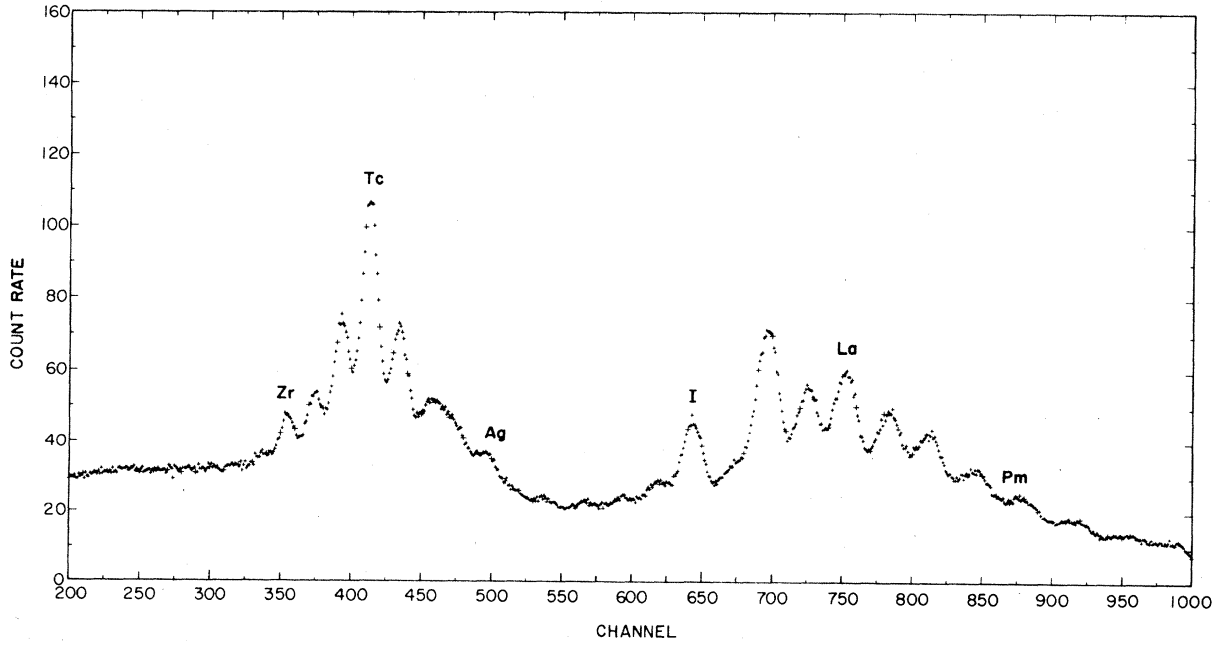

FIG. 6. X rays in coincidence with fission of Cf^{252} and electrons above 50 keV. The energy calibration is the same as in Fig. 5. Several of the $K\alpha$ energies have been labeled for the convenience of the reader.

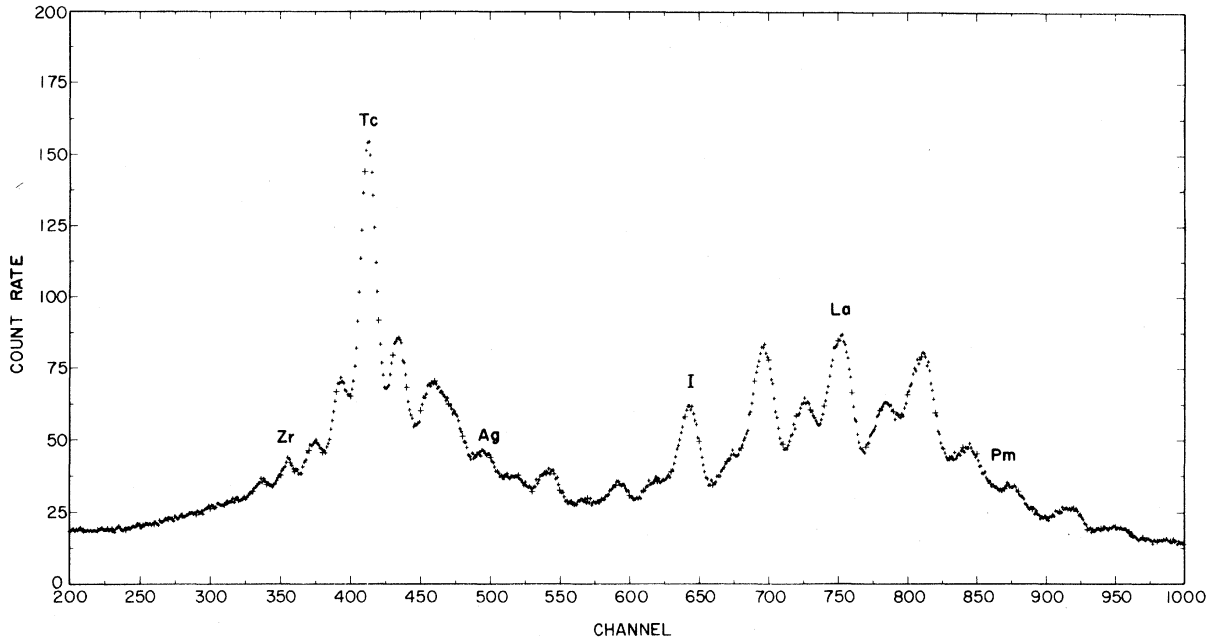

FIG. 7. X rays in coincidence with only electrons above 50 keV. The energy calibration is the same as in Fig. 5. Several of the $K\alpha$ energies have been labeled for the convenience of the reader.

mal-neutron fission of U^{235}.

A significant change in the low-energy background is also evident. Some decrease in the background of the spectrum in Fig. 6 from that of Fig. 5 is observable. This decrease is expected since requiring an electron coincidence will reduce the acceptance of Compton scattered γ rays which have been backscattered from the chamber walls. A much larger decrease in the low-energy background of the x-ray–electron coincidence spectrum from the other two spectra is evident, probably reflecting a larger x-ray-to-γ-ray yield for the decay products.

B. Electron Spectra

The electron data were sorted to give an electron spectrum for each element produced in fission. Minimum and maximum channel numbers were assigned about each peak in the x-ray spectra, and electrons which were coincident with x rays falling within each range of channels were grouped together and then sorted by electron energy. The minimum and maximum channel numbers were assigned to each peak so as to minimize the contributions from the x rays of adjacent elements and where possible from $K\beta$ x rays.

The same channel ranges were used to sort both the x-ray–electron–fission coincident data and the x-ray–electron coincident data. The total electron spectrum (electron spectrum in coincidence with all x rays) for the x-ray–electron–fission coincidence experiment and the total electron spectrum for the x-ray–electron coincidence experiment showed almost no structure, indicating many closely spaced unresolved electron lines. The second spectrum does, however, show two peaks at 307 and 725 keV. Analysis of the electron spectrum for each element showed that these peaks are from high-yield lines of indium (307 keV) and molybdenum (725 keV).

A typical spectrum from the x-ray–electron–fission coincident experiment is shown in Fig. 8 ($_{44}$Ru). A rather intense peak is evident at 219 keV. At this energy, the peak exhibits a large tail consistent with the results of the distributed calibration source measurements. Electrons of approximately this energy have been observed by Atneosen and Thomas[12] in coincidence with fragments of mass $A = 109 \pm 2$ and by Bowman *et al.*[1] in coincidence with fragments of mass $A = 110 \pm 1$, atomic weights over which $_{44}$Ru is predicted to have a high

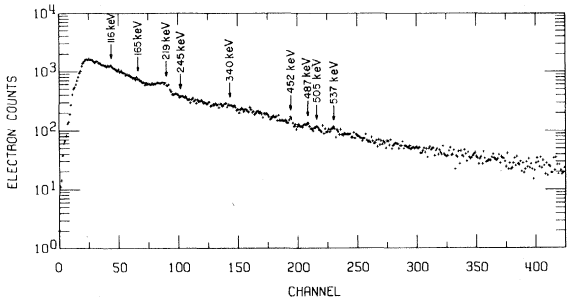

FIG. 8. Spectrum of electrons in coincidence with fission and $K\alpha$ x rays from $_{44}$Ru.

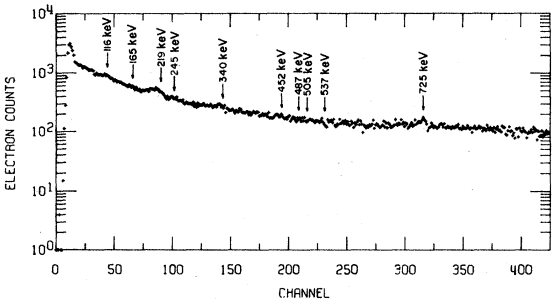

FIG. 9. Spectrum of electrons in coincidence with $K\alpha$ x rays from $_{44}$Ru.

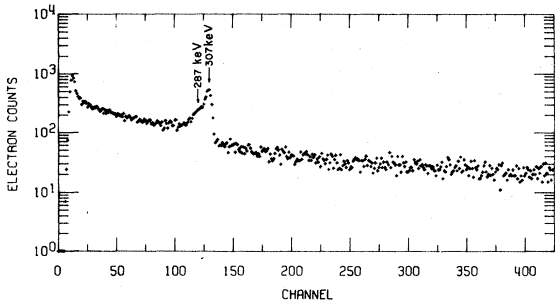

FIG. 10. Spectrum of electrons in coincidence with $K\alpha$ x rays from $_{49}$In.

yield. More recently, Watson *et al.*[13] have measured a 218-keV electron from $_{44}$Ru and have assigned an atomic weight of 110 to the isotope. Cheifetz *et al.*[19] have measured the energy of the γ transitions from the 2^+ to ground state for the light even-even nuclei produced in the fission of Cf^{252} and has found γ transitions at 242.3, 240.8, and 236.8 keV from Ru^{108}, Ru^{110}, and Ru^{112}, respectively, with Ru^{110} having the highest yield.

Several less-intense peaks are observable in the spectrum shown in Fig. 8. In order to minimize the chances of mistaking statistical fluctuations as peaks, each of the three runs was analyzed separately and a peak was not accepted unless it appeared in at least two out of the three runs. In addition, the peaks were required to meet the expected shapes as determined by the distributed calibration sources.

Some electrons from the complementary Z fragments will be observable in the spectrum of interest since there is some probability that both fragments will undergo an internal conversion transition. Since this probability is in general small, the intensity of the electron lines from the complementary Z fragments will be reduced to less than 30% in the normal spectrum compared to their appearance in the corresponding complementary Z spectrum. Thus by comparing the spectrum of interest with that of the complementary Z spectrum, electron lines from the complementary Z fragments could be eliminated.

Figure 9 is an electron spectrum of the same element, $_{44}$Ru, for the x-ray–electron coincident experiment. Many of the same features are noted. This spectrum contains the same lines as the triple-coincidence spectrum, since both prompt x rays and decay x rays are recorded. An additional peak at 725 keV is observed. Since this peak is not observable in Fig. 8, it is most likely due to an isotope produced by β decay. Further analysis showed that this peak is in coincidence with the $_{42}$Mo $K\beta$ x rays whose energy is approximately the same as that of $K\alpha$ x rays of $_{44}$Ru.

An attempt was also made to identify the isotope producing each electron line by comparison to known decay schemes. Unfortunately very little knowledge of the decay schemes exists for the neutron-excess rare-earth fission fragments and so identification of isotopes is not generally possible. In some cases, however, it was possible to identify the isotopes producing electron lines for the decay products observed in the x-ray–electron experiment. The strong line at 307 keV and a weaker line at 287 keV in the electron spectrum of indium shown in Fig. 10 appear to be produced by In^{115} and In^{117}, respectively.

Figures 5, 6, and 7 illustrate that more of the observed transitions occur in odd-Z elements than even-Z elements, apparently due to the high energy of the first excited state in even-even nuclides. The higher x-ray yield of odd-Z elements is most pronounced in the heavy fragment peak of the spectrum of Fig. 7 which includes the contribution from fission products. These fission products are somewhat lighter than the pre-β-decay fragments of the same Z, and hence are farther from regions of stable deformation (a region characterized by lower first excited states). The even-even fission products are thus expected to have first excited states of higher energy than those of the pre-β-decay fragments reducing the probability of an internal conversion transition.

In spite of this there is some evidence of even-even transitions. Watson *et al.*[13] have measured a 241-keV γ transition and have assigned the transition to the first excited state of Ru. In addition, Cheifetz *et al.*[19] have measured three γ transitions occurring at 242.3, 240.8, and 236.8 keV which they have assigned to the first excited state to ground transition of Ru^{108}, Ru^{110}, and Ru^{112}, respectively. A strong 241-keV transition in Ru has also been observed in this work. The 2^+ to 0^+ transitions reported by Cheifetz *et al.*[19] for Zr^{100}, Mo^{104}, Pd^{114}, and Pd^{116}, and by Watson *et al.*[13] for Ba^{144} are also observed in this experiment.

This work has complemented and confirmed pre-

vious measurements, and has presented new data which needs further investigation. Work on the determination of the radiation backgrounds is being undertaken in order to accurately determine the x-ray and electron yields measured in this experiment. We are also investigating methods to determine the effect of the partly filled electronic shells on the ratio of $K\beta$ x rays to $K\alpha$ x rays. Similar measurements are also being started for the thermal-neutron fission of U^{235}. It is anticipated that all of these measurements will help in the understanding of the results presented here.

ACKNOWLEDGMENTS

The authors would like to express their appreciation to T. Ganley, S. Hinata, and C. Withee for their assistance with the experiments, and to S. Barnes, J. Goldman, and R. Harrison for construction of the vacuum chamber.

---

†Research supported by a grant from the National Science Foundation.

*The material in this article is based upon a dissertation by one of the authors (N.L.S.) submitted in partial fulfillment of the requirements for the doctoral degree at the University of Illinois.

‡Present address: Combustion Engineering, Windsor, Connecticut.

[1]H. R. Bowman, S. G. Thompson, R. L. Watson, S. S. Kapoor, and J. O. Rasmussen, University of California Radiation Laboratory Report No. UCRL-11902, 1965 (unpublished).

[2]S. S. Kapoor, H. R. Bowman, and S. G. Thompson, Phys. Rev. 140, B1310 (1965).

[3]L. E. Glendenin and J. P. Unik, Phys. Rev. 140, B1301 (1965).

[4]E. M. Bohn, B. W. Wehring, and M. E. Wyman, Appl. Phys. Letters 12, 199 (1968).

[5]S. S. Kapoor, V. S. Ramamurthy, and R. Zaghloul, Phys. Rev. 177, 1776 (1969).

[6]J. E. Canty, C. D. Coryell, L. Leifer, and N. C. Rasmussen, Bull. Am. Phys. Soc. 10, 481 (1965).

[7]W. John, R. Massey, and B. G. Saunders, Phys. Letters 24B, 336 (1967).

[8]W. John, D. H. White, B. G. Saunders, R. W. Jewell, and D. Groves, Arkiv Fysik 36, 287 (1966).

[9]B. W. Wehring and M. E. Wyman, Phys. Rev. 157, 1083 (1967).

[10]R. L. Watson, H. R. Bowman, and S. G. Thompson, Phys. Rev. 162, 1169 (1967).

[11]L. E. Glendenin, H. C. Griffin, W. Reisdorf, and J. P. Unik, in *Proceedings of the Second International Atomic Energy Symposium on Physics and Chemistry of Fission, Vienna, Austria, 1969* (International Atomic Energy Agency, Vienna, Austria, 1969).

[12]R. A. Atneosen and T. D. Thomas, Phys. Rev. 148, 1206 (1966).

[13]R. L. Watson, J. B. Wilhelmy, R. C. Jared, C. Rugge, H. R. Bowman, S. G. Thompson, and J. O. Rasmussen, Nucl. Phys. A141, 449 (1970).

[14]N. L. Shapiro, B. W. Wehring, and M. E. Wyman, unpublished.

[15]B. W. Wehring, P. E. Rohan, N. L. Shapiro, and M. E. Wyman, Nucl. Instr. Methods 66, 330 (1968).

[16]E. J. Williams, Proc. Roy. Soc. (London) A125, 420 (1929).

[17]L. Landau, J. Phys. (USSR) 8, 201 (1944).

[18]A. H. Wapstra, G. J. Nijgh, and R. Van Liehout, *Nuclear Spectroscopy Tables* (North-Holland Publishing Company, Amsterdam, The Netherlands, 1959).

[19]E. Cheifetz, R. C. Jared, S. G. Thompson, and J. B. Wilhelmy. Phys. Rev. Letters 25, 38 (1970).